ACS APPLIED MATERIALS & INTERFACES

Research Article

www.acsami.org

All-Solid-State Reduced Graphene Oxide Supercapacitor with Large Volumetric Capacitance and Ultralong Stability Prepared by Electrophoretic Deposition Method

Mei Wang,[†] Le Dai Duong,[†] Nguyen Thi Mai,[†] Sanghoon Kim,[†] Youngjun Kim,[‡] Heewon Seo,[‡] Ye Chan Kim,[†] Woojin Jang,[‡] Youngkwan Lee,[§] Jonghwan Suhr,[†,‡] and Jae-Do Nam*[,†,‡]

[†]Department of Energy Science, Sungkyunkwan University, Suwon 440-746, South Korea

[‡]Department of Polymer Science and Engineering, Sungkyunkwan University, Suwon 440-746, S. Korea

[§]Department of Chemical Engineering, Sungkyunkwan University, Suwon 440-746, S. Korea

Supporting Information

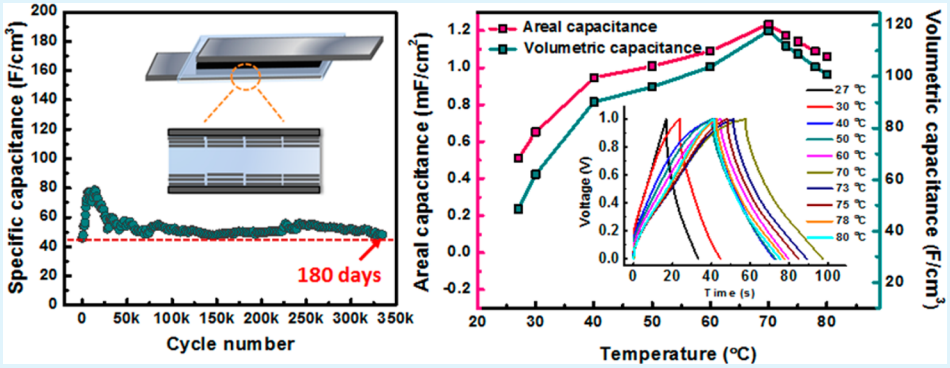

ABSTRACT: Portable energy storage devices have gained special attention due to the growing demand for portable electronics. Herein, an all-solid-state supercapacitor is successfully fabricated based on a poly(vinyl alcohol)-H_3PO_4 (PVA–H_3PO_4) polymer electrolyte and a reduced graphene oxide (RGO) membrane electrode prepared by electrophoretic deposition (EPD). The RGO electrode fabricated by EPD contains an in-plane layer-by-layer alignment and a moderate porosity that accommodate the electrolyte ions. The all-solid-state RGO supercapacitor is thoroughly tested to give high specific volumetric capacitance (108 F cm^{-3}) and excellent energy and power densities (7.5 Wh cm^{-3} and 2.9 W cm^{-3}, respectively). In addition, the all-solid-state RGO supercapacitor exhibits an ultralong lifetime for as long as 180 days (335 000 cycles), which is an ultrahigh cycling capability for a solid-state supercapacitor. The RGO is also tested for being used as a transparent supercapacitor electrode demonstrating its possible use in various transparent optoelectronic devices. Due to the facile scale-up capability of the EPD process and RGO dispersion, the developed all-solid-state supercapacitor is highly applicable to large-area portable energy storage devices.

KEYWORDS: *solid-state supercapacitor, RGO, EPD, volumetric capacitance, volumetric energy density*

INTRODUCTION

Long lifetime and high specific capacitance are the most critical issues for supercapacitors. Although electrochemical double layer capacitors (EDLCs) can deliver long cycling life, but their specific capacitance is limited.[1,2] The pseudocapacitor materials such as conductive polymers and metal oxides give high specific capacitance, but their performances are usually limited within only a few thousand cycles due to their poor long-term stability. It should be mentioned that the long-term cycling behavior of supercapacitors is expected for practical applications, say, over 100 000 cycles, which can hardly achieved for those pseudocapacitors.[3]

Ensuring the long life cycle of supercapacitors, graphene-based nanomaterials for EDLC electrodes have recently attracted significant interests due to their unique characteristics, such as light weight, high electrical conductivity, and large electrochemical surface area. However, graphene sheets have extremely high surface energies, so they easily coagulate themselves during the electrode fabrication process. Therefore, one of the key issues to fabricate graphene electrode materials is to minimize restacking of the graphene sheets to maximize the exposed surface area of graphene sheets for a facile transport of electrolyte ions. Some supercapacitor electrodes made from porous graphene (or reduced graphene oxide (RGO)) electrodes often give high gravimetric capacitance[4−7] stemming from the large void volume of those porous structures. However, they usually provide smaller volumetric capacitance than the commercialized activated carbon electrodes due to the

Received: November 9, 2014
Accepted: December 29, 2014
Published: December 29, 2014

DOI: 10.1021/am507656q
ACS Appl. Mater. Interfaces 2015, 7, 1348−1354

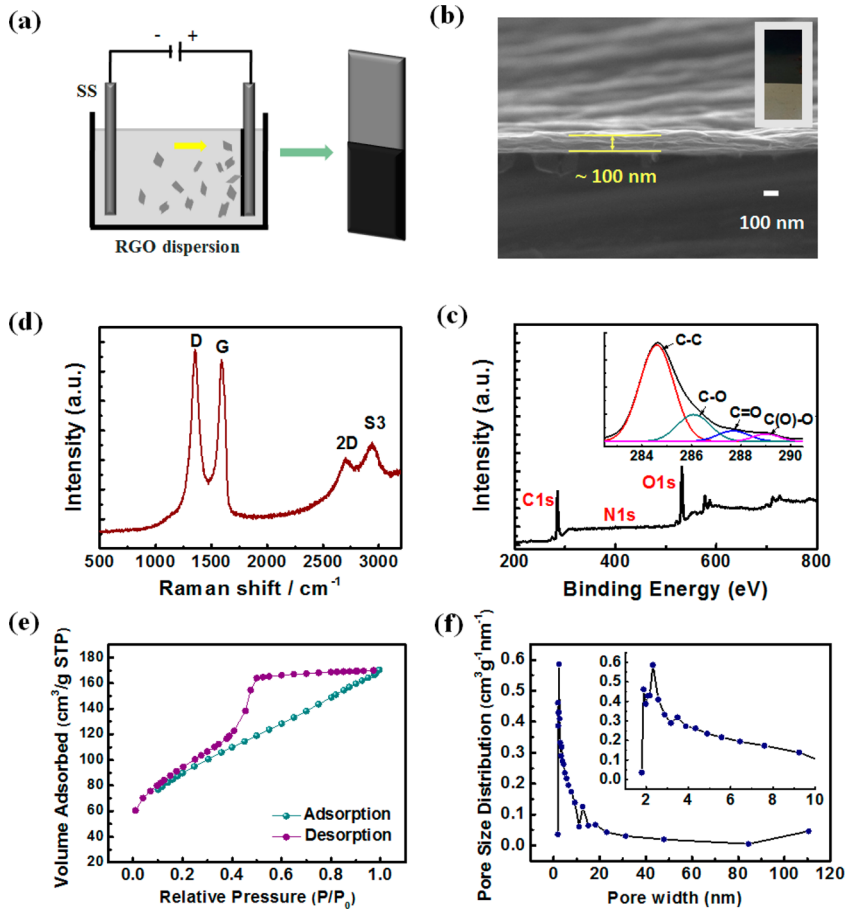

Figure 1. (a) Schematic representation of the anodic EPD process of RGO. (b) SEM image of cross-sectional RGO membrane, showing the layer-by-layer morphology with thickness of ∼100 nm. (c) XPS data of RGO membrane electrode; (inset) narrow scan spectra. (d) Raman spectrum of RGO membrane at excitation wavelength of 514 nm. (e) Nitrogen adsorption and desorption isotherms of RGO, showing the presence of meso- and micropores. (f) Pore size distribution of RGO electrode material; (inset) micro- and mesopore size distribution obtained by the BJH method.

enormous voids and poor packing densities of crispy graphene granules.[8]

In commercial supercapacitors, electrodes and separators are usually immersed in the liquid electrolytes and subsequently packaged into cylindrical containers or coin cells. However, increasing demand for portable electronics has spawned different interests and requirements among material researchers in their quest for more compatible and safer energy storage devices.[9−11] In the advent of many flexible devices, particularly, the liquid-state electrolyte makes it extremely hard for the supercapacitors to be incorporated into those flexible devices due to the electrolyte leakage and difficulties in automated assembly processes. In this sense, the solid-state electrolyte has been considered as a desirable alternative. Poly(vinyl alcohol) (PVA) is a polymer-electrolyte that can be applied to solid-state energy-storage device usually utilized in a form of mixtures with strong acids, such as sulfuric acid and phosphoric acid. Due to its hydrophilic and stable characteristics, the PVA−H_3PO_4 polymer membrane could work as a solid-state electrolyte and electrical separator in supercapacitors. Compared with the aqueous electrolyte system, the PVA−H_3PO_4 electrolyte system can reduce the device thickness and weight desirably simplifying the fabrication process by eliminating the needs for packaging materials and equipment.[2] Based on our previous work on an RGO membrane prepared by the electrophoretic deposition (EPD) method,[12] the interlayer distance of the RGO sheets become 6.66 Å, which may accommodate $H_2PO_4^-$, HPO_4^{2-}, and PO_4^{3-} ions in the size of ca. 4.8 Å to be used as solid-state supercapacitor electrodes.[13]

In this study, we develop an efficient EPD method to prepare an RGO membrane in a layer-by-layer structure of RGO sheets. In our all-solid-state supercapacitor, the RGO membrane works as electrodes and the PVA−H_3PO_4 as the polymer electrolyte and separator. The electrochemical performance of the as prepared RGO supercapacitor was tested; it showed markedly high specific volumetric capacitance, long cycle ability, and high energy and power densities.

EXPERIMENTAL SECTION

Material Preparation. Graphite oxide was synthesized by the oxidation of graphite with the modified Hummers method.[14] Five grams of graphite flakes was mixed with a mixture of concentrated H_2SO_4 (180 mL) and H_3PO_4 (20 mL). After the mixture stirred for 1 h, 15 g of potassium permanganate was added, and the mixture was oxidized for 2 h at 50 °C. Then, 300 mL of deionized (DI) water and H_2O_2 at a ratio of 9:1 was added into the mixture and stirred for 30 min to remove impurities. Subsequently, the graphite oxide was washed with DI water several times and collected by centrifugation.

To prepare the graphene oxide dispersion, 0.1 g graphite oxide powder was dispersed in 100 mL of DI water by ultrasonication for 4 h, followed by centrifugation at 4000 rpm for 15 min to remove the unexfoliated graphite oxide flakes. The resulting GO dispersion was reduced by the rate-controlled reduction method to prepare a stable RGO dispersion.[15] The GO dispersion was put into an ice bath and

DOI: 10.1021/am507656q
ACS Appl. Mater. Interfaces 2015, 7, 1348−1354

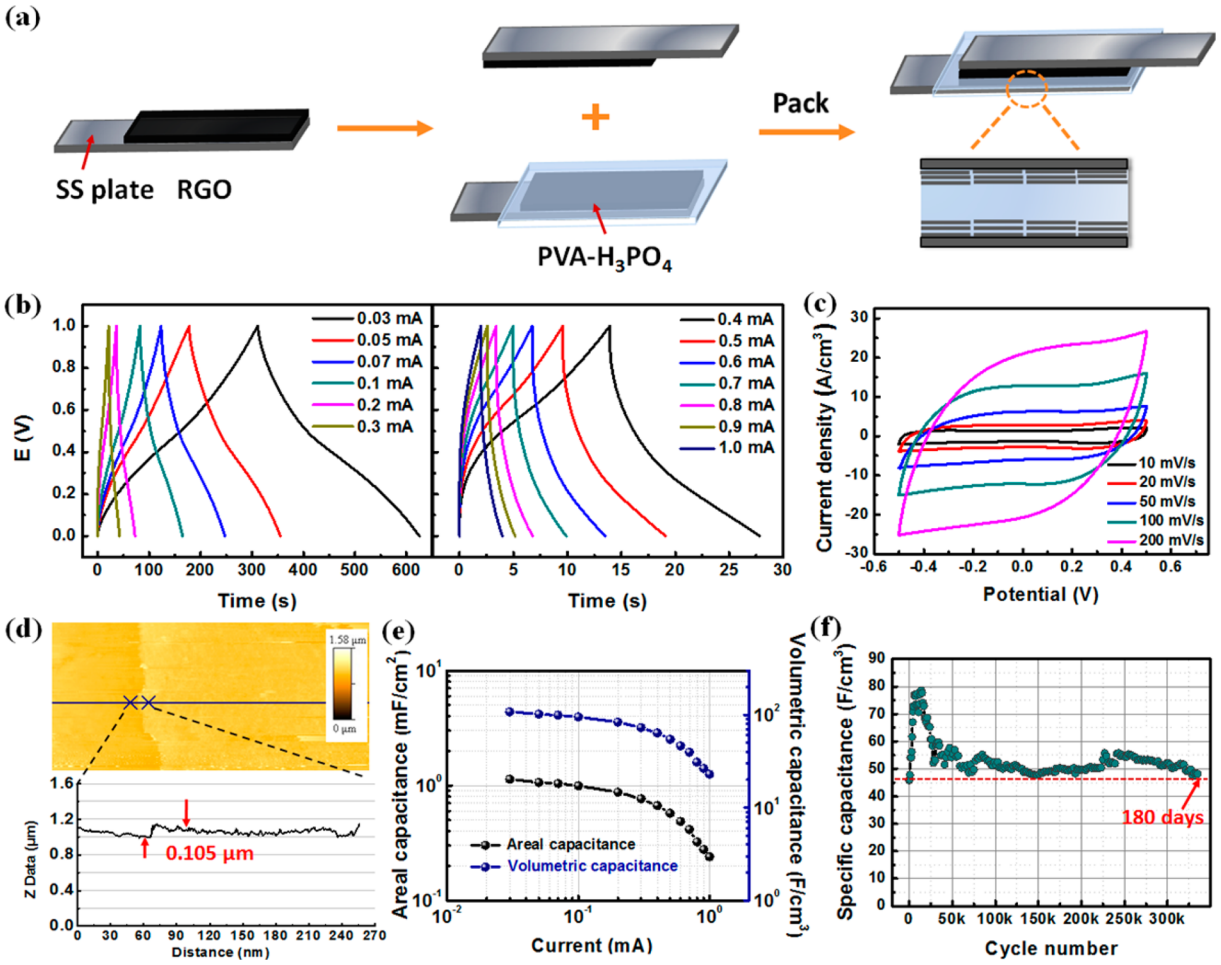

Figure 2. (a) Schematic representation of the fabrication process of RGO all-solid-state supercapacitor. (b) Galvanostatic CD curves in the current range of 0.03−1.0 mA. (c) CV curves of the all-solid-state supercapacitor at scan rates of 10, 20, 50, 100, and 200 mV/s. (d) AFM image and the height profile of the RGO membrane. The thickness of the representative stacked film is 0.105 μm. (e) Specific areal and volumetric capacitance values of RGO membrane electrode calculated from galvanostatic curves as a function of applied CD current density. (f) Cycle ability test of all-solid-state supercapacitor measured by CD at the current of 0.2 mA. The test was carried out for as long as 180 days.

cooled down to 0−5 °C, and then 20 mL of 5 mM hydrazine solution was added. Afterward, the suspension was heated on a flat heater at 200 °C for 30 min. During the reduction process, the suspension was stirred with a magnetic bar. The EPD of RGO was directly carried out in the RGO aqueous suspension at room temperature. RGO dispersion (100 mL, 1.0 mg/mL) was placed into a beaker, and two stainless steel (SS) plates were immersed into the suspension as the EPD electrodes. A direct-current voltage of 3 V was applied to SS electrodes for 5 min, and subsequently, RGO flakes were deposited onto the anode electrode. The magnetic stirrer was applied to the RGO suspension during EPD process. Then, the RGO deposited SS substrate was pulled out from the suspension, washed with DI-water, and dried overnight in air at room temperature.

The PVA−H_3PO_4 electrolyte was prepared by mixing 1 g of poly(vinyl alcohol) (99%) powder with 10 mL of DI water. The mixture was subsequently heated to 90 °C until the solution became clear. The solution was stirred by a magnetic bar. After the solution was cooled to room temperature, 0.8 g of concentrated phosphoric acid was added into the PVA solution, and the solution was stirred for 2 h. Finally, the viscous solution was cast into a Petri dish and dried at room temperature. After 48 h, the polymer electrolyte became hard, and the hardened electrolyte was cut into pieces of the same size as that of the electrodes.[16]

Characterization. The morphology of the RGO membrane was characterized by field emission scanning electron microscopy (FE-SEM, JEOL, JEM 7000F, Japan). X-ray photoelectron spectroscopy (XPS, QUANTUM 2000, Physical Electronics, Inc., Chanhassen, MN) was performed using focused monochromatized Al Kα radiation ($h\nu$ = 1486.6 eV). Raman spectroscopy (Renishaw, RM-1000 Invia) was performed with excitation energy of 2.41 eV and wavelength of 514 nm (Ar^+ ion laser). The specific surface area of the EPD RGO membrane was determined using the BET equation with nitrogen gas at 77 K (Micrometrics ASAP 2020). The pore volume and the pore size distribution were calculated using the Barrett−Joyner−Holenda (BJH) model. Atomic force microscopy (AFM, Bruker, Innova) was used to measure the thickness of the RGO membrane. Cyclic voltammetry (CV), galvanostatic charge/discharge (CD) and electrochemical impedance spectroscopy (EIS) were obtained by a multichannel potentiostat and a multichannel galvanostat (Bio-Logic Science Instruments, VMP3). RGO sheets were used as the supercapacitor electrodes, the SS substrate as the current collector, and PVA−H_3PO_4 as both the electrolyte and separator. The packing density of EPD prepared RGO in this study is 0.76 g cm^{-3}. The mass loadings of each single RGO electrode material are 168 μg (electrode area of 1.6 cm^2, thickness of 1378 nm), 33 μg (electrode area of 4.16 cm^2, thickness of 105 nm), and 1 μg (electrode area of 1.35 cm^2, thickness of 10 nm).

RESULTS AND DISCUSSION

Figure 1a shows a schematic representation of the anodic EPD process of RGO. When a voltage is applied to the stainless steel (SS) current collector, the RGO flakes with negative charges, which originate from the oxygen-containing functional groups,

DOI: 10.1021/am507656q
ACS Appl. Mater. Interfaces 2015, 7, 1348−1354

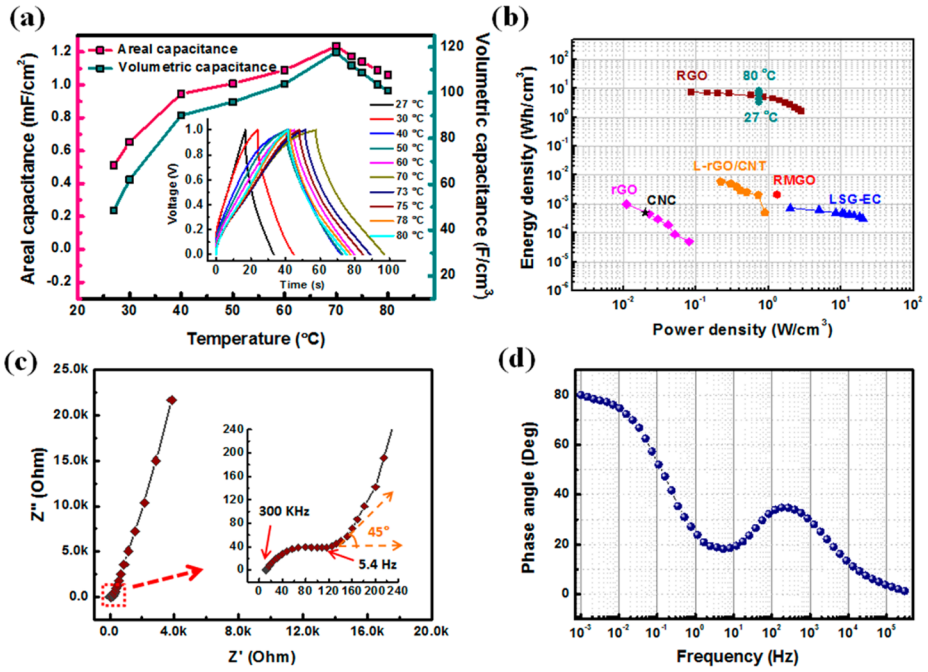

Figure 3. (a) Areal and volumetric capacitance changes as a function of temperature (27−80 °C), (inset) galvanostatic CD curves of various temperatures. (b) RGO all-solid-state supercapacitor compared with various carbon-based supercapacitors in literature by the Ragone plot; LSG-EC, laser-scribed graphene electrochemical capacitor;[2] RMGO, reduced multilayer graphene oxide;[13] rGO, reduced graphene oxide; L-rGO/CNT, multistacked rGO/CNT;[20] and CNC, carbon nanocups.[24] (c) Nyquist plot of RGO membrane electrode for the frequency range from 300 kHz to 1 mHz, and (inset) details of the high-frequency region. (d) Phase angle versus frequency for RGO all-solid-state supercapacitor measured in the frequency range of 300 kHz to 1 mHz.

move to the anode and stack tightly onto the surface of the SS substrate in the in-plane direction. The in-plane direction stacking by the electric field force results in the high in-plane conductivity of the RGO membrane.[17] Figure 1b and Figure S1 (Supporting Information) show cross-sectional image of the RGO membrane fabricated by EPD; the RGO layers stack in the in-plane direction as a layer-by-layer structure. As shown in Figure 1b, the thickness of the RGO membrane is around 100 nm.

As presented in Figure 1c, the XPS C 1s and O 1s spectra of RGO indicate a carbon content of 67.7% and a high oxygen content of 31.3% in the RGO, with an O/C ratio of 0.46, which indicates a partial reduction of the RGO. The narrow scan spectrum (Figure 1c, inset) shows that the C 1s peak is composed of four Gaussian peaks with binding energies of 284.6 eV (nonoxygenated C rings, −C═C−/−C−C−), 286.1 eV (epoxy and hydroxyl, −C−O−), 287.7 eV (carbonyl, −C═O), and 289.0 eV (carboxyl, −O−C═O).[17] These results demonstrate that a certain amount of the oxygen-containing functional groups remained in the RGO layers, ensuring the stability of the RGO suspension and the anodic deposition of the RGO membrane on positive electrode. The Raman spectrum of the RGO membrane prepared using EPD is presented in Figure 1d. Similar to the result in the previous work, D-band at 1351 cm^{-1}, G-band at 1588 cm^{-1}, and 2D-band at 2706 cm^{-1} appear in the spectrum, demonstrating specific graphene characteristics.[17] The high D-band intensity with an intensity ratio of D- and G-band (I_D/I_G) at 1.05 indicates the amount of defects generated during the graphite oxidation and reduction processes.

The nitrogen adsorption and desorption isotherms of the RGO membrane measured at 77 K are shown in Figure 1e, indicating the presence of meso- and micropores. The curve illustrates a rapid uptake in the p/p_0 region of <0.4 followed by a representative "type IV" hysteresis in the mesopore region, revealing that the RGO membrane fabricated by EPD contained mesopores with a minor fraction of micropores, which was demonstrated by the pore size distribution obtained by the BJH method (Figure 1f and Figure S2, Supporting Information).[18] The BET specific surface area and pore volume of the RGO are 304.4 $m^2\ g^{-1}$ and 0.25 $cm^3\ g^{-1}$, respectively.

Figure 2a shows a schematic representation of the fabrication process of the all-solid-state RGO supercapacitor. The PVA−H_3PO_4 electrolyte, working as both an electrolyte and a separator, was placed and packed between two RGO electrode pieces. The electrochemical performance of the RGO all-solid-state supercapacitor was analyzed using CV and galvanostatic charge/discharge (CD). Figure 2b shows the CD curves of the all-solid-state supercapacitor in the current range of 0.03−1 mA (0.69−22.89 A cm^{-3}). The CD curves are close to triangle shape, which confirms the formation of an efficient electrical double layer (EDL) and the good charge propagation across the two RGO electrodes.[13] Characterizing the CV capacitive behavior of our RGO electrode material, as shown in Figure 2c, the CV curves have a quasi-rectangular shape with little variance, even at high scan rates, indicating that efficient EDLs are established in the RGO electrodes. For the calculation of the specific capacitance of a supercapacitor, the capacitance based on the gravimetric value is usually used. Because the mass of the RGO electrode is so small, we calculated the capacitance based on the geometrical area (or volume) of the electrode to avoid dealing with the accuracy required in measuring the electrode mass. The specific areal capacitance (C_A) and volumetric capacitance (C_{vol}) are calculated as follows:

DOI: 10.1021/am507656q
ACS Appl. Mater. Interfaces 2015, 7, 1348−1354

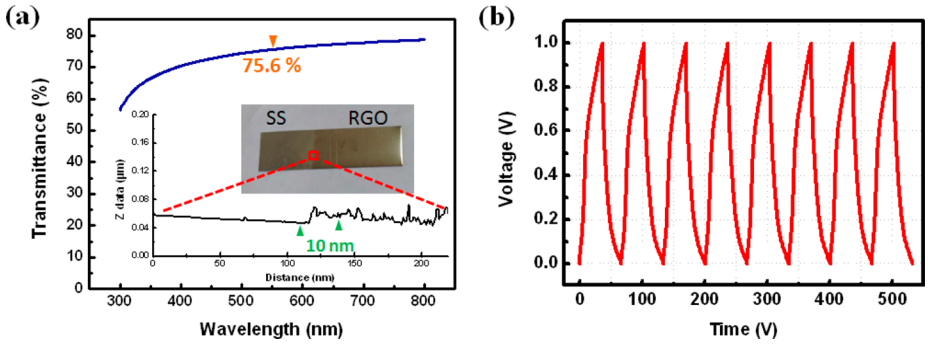

Figure 4. (a) UV−vis spectrum of transparent RGO membrane fabricated by EPD, with transmittance of 75.6% at wavelength of 550 nm; (inset) digital photograph of RGO and the AFM height profile of the transparent RGO film, showing a thickness of 10 nm. (b) Galvanostatic CD measurement of all-solid-state supercapacitor with transparent RGO electrode at 0.01 mA.

$$C_A = \frac{I\Delta t}{2A\Delta U},\ C_{vol} = \frac{I\Delta t}{2V\Delta U} \quad (1)$$

where I is the discharge current, Δt is the discharge time, ΔU is the voltage range, and A and V are the area and volume, respectively, of one single electrode material. To obtain the volumetric capacitance, we measured the thickness of the RGO membrane by AFM. Multiple cross sections were recorded, and a number of step heights were measured. Figure 2d shows an AFM image of the RGO membrane and the height profile along the black line across the sample. Based on the height profile shown in Figure 2d, the RGO has an average thickness of 0.105 μm.

Figure 2e compares the specific areal capacitance and volumetric capacitance for the current range of 0.03−1 mA (0.69−22.89 A cm^{-3}). At the current density of 0.69 A cm^{-3}, the all-solid-state supercapacitor has a volumetric capacitance as high as 108 F cm^{-3} (gravimetric capacitance of 142 F g^{-1}), which is larger than the capacitance values of graphene-based EDLCs appearing in literature.[2,5,19−22] As shown in Figure 2e, as with all the EDLCs, the capacitance values gradually decrease as the current density increases, but the volumetric capacitance reaches 23 F cm^{-3} at the current density of 22.89 A cm^{-3}, which compares well with the values reported in literature.[2,19,20] The high capacitance originates from the large active surface area, as well as the in-plane stacked structure, of the RGO membrane, which may very well provide excellent electrode conductivity.[17] In addition, our RGO electrodes fabricated by the EPD process are binder-free and thus give a substantially reduced interfacial resistance. We believe that the developed methodology enables the full utilization of the active surface area of the RGO sheets stacked well in the in-plane direction of the electrode, which subsequently leads to facile transport of $H_2PO_4^-$, HPO_4^{2-}, and PO_4^{3-} ions.

Figure 2f shows the specific volumetric capacitance as a function of cycle number of times (specific areal capacitance as a function of cycle number in Figure S3, Supporting Information). The specific capacitance was extracted from the galvanostatic charge/discharge (CD) curves. It is interesting to note that the specific capacitance sharply increases up to the initial 6000 cycles, due to the improved surface wetting of the RGO electrode with the electrolyte and the electrochemical reduction of the RGO during the charge/discharge process.[23] After the 15 000th cycle, the capacitance starts decreasing due to the reduced ion mobility in the electrolyte by the evaporation of the water in the polymer electrolyte. From the 27 000th to the 335 000th cycle, the capacitance is leveled off with little variance. It is worth noting that our all-solid-state supercapacitor is stable for as long as 180 days (335 000 cycles), maintaining a the specific capacitance still larger than that at the first cycle. This performance demonstrates the ultralong cycle ability of our all-solid-state supercapacitor.

The temperature effect on the capacitance values (areal and volumetric capacitances) and CD behaviors of our all-solid-state supercapacitor are explored in Figure 3a. Compared to the capacitance measured at room temperature (27 °C), the specific capacitance increases with temperature up to 70 °C, which is believed to be due to the molecular alignment of PVA chains and the excitation of the charge carriers present on the imperfect sites of the electrode material surface with a moderate temperature increase.[24] When the supercapacitor is heated over 70 °C, the capacitance performance starts degrading due to the overevaporation of water in the polymer electrolyte.

To demonstrate the energy storage capability of our all-solid-state supercapacitor, we show in Figure 3b a Ragone plot as compared with the literature values. The specific energy and power are evaluated in this study as follows:

$$E = \frac{C_V(\Delta U)^2}{2},\ P = \frac{E}{\Delta t} \quad (2)$$

The volumetric energy density of the RGO all-solid-state supercapacitor reaches up to 7.5 W h cm^{-3} (at the power density of 0.1 W cm^{-3}) and gradually decreases to 1.6 W h cm^{-3} (at the power density of 2.9 W cm^{-3}), which is much higher than the reported values of other graphene-based supercapacitors.[2,13,20,24] Additionally, our all-solid-state supercapacitor exhibits an increment in energy density from 27 °C (3.4 W h cm^{-3}) to 80 °C (7.0 W h cm^{-3}).

We further investigated the performance of our RGO supercapacitor using a Nyquist plot (Figure 3c). Excellent capacitive behavior and a small internal resistance are also exhibited in the inset of Figure 3c. The impedance curve intersects the x-axis at a 45° angle, indicating that the porous electrode is saturated with electrolyte.[25] The equivalent series resistance (ESR) of the RGO obtained from the x intercept of the Nyquist line in the low-frequency region is 132 Ω (Figure 3c, inset). It should be noticed that a semicircle appears in the high frequency region. It is believed to be caused by the charge transfer resistance, which usually stems from the poor ionic conductivity at the interfaces between the electrodes and the solid-state electrolyte.[26] The knee frequency is 5.4 Hz, which indicates the applicability of our RGO all-solid-state supercapacitor.[4] In the low-frequency region, a vertical line should be

DOI: 10.1021/am507656q
ACS Appl. Mater. Interfaces 2015, 7, 1348−1354

observed with decreasing frequency in theory, but in reality, there is usually some deviation due to the electrode properties such as electrode porosity and electrode roughness. The Nyquist plot of our supercapacitor is not a rigorous vertical line due to the pore size distribution of the RGO electrode. The phase angle of the supercapacitor is about 80° at a frequency of 1 mHz, which is close to the 90° of ideal capacitors, as shown in Figure 3d. Although the capacitor-to-inductor transition occurs as the frequency increases, showing a strong response between 200 and 3000 Hz, our RGO supercapacitor retains its capacitance characteristics.[26]

In addition, as shown in Figure 4a, the performance of a supercapacitor with a thin 10 nm EPD-prepared RGO electrode is presented. The UV−vis spectrum of the RGO membrane shows a transmittance of 75.6% at the wavelength of 550 nm. The RGO membrane is prepared by transferring it onto a glass slide using the chemical detaching method previously published by our group.[17] The galvanostatic CD measurement (Figure 4b) shows a slightly distorted triangular CD profile and exhibits a high volumetric capacitance of 114 F cm^{-3} of the RGO supercapacitor (gravimetric capacitance of 150 F g^{-1}), demonstrating the capability of the RGO membrane to be utilized as transparent supercapacitors. Furthermore, the capacitive performances of our RGO all-solid-state supercapacitor as a function of RGO electrode thickness are also investigated (Figure S5, Supporting Information). The volumetric capacitance of the RGO all-solid-state supercapacitors decreases moderately with the increased film thickness due to the limited infiltration of the gel electrolyte.[27]

CONCLUSIONS

In summary, we report the synthesis of a layer-by-layer RGO membrane that is directly deposited on the current collector as a supercapacitor electrode. Packed with the PVA−H_3PO_4 electrolyte and separator, our all-solid-state supercapacitor exhibited high volumetric capacitance and energy density and an ultralong lifetime. Due to the lamellar packaging of RGO sheets, the RGO membrane had high conductivity and saved electrode space. We also demonstrated the possibility of fabricating a transparent supercapacitor with an RGO electrode fabricated by EPD, in which RGO sheets are packed in-plane to form an excellent supercapacitor electrode. Because EPD is scalable, it is highly applicable in preparing large-scale supercapacitors. The simplicity of the device fabrication process and the desirable supercapacitor performance support the application of the all-solid-state RGO supercapacitors as large-area, portable, and transparent supercapacitors. Further study and optimization of this process will be reported in the future.

ASSOCIATED CONTENT

Supporting Information

Additional plots of cumulative pore volume as a function of pore width, cycle ability test in terms of specific areal capacitance, areal and volumetric capacitances as functions of frequency, and the real and imaginary parts of specific volumetric capacitance versus frequency of the all-solid-state supercapacitor. This material is available free of charge via the Internet at http://pubs.acs.org.

AUTHOR INFORMATION

Corresponding Author

*E-mail: jdnam@skku.edu. Tel.: +82-31-290-7285. Fax: +82-31-292-8790.

Author Contributions

The manuscript was written through contributions of all authors. All authors have given approval to the final version of the manuscript.

Notes

The authors declare no competing financial interest.

ACKNOWLEDGMENTS

This research was supported by research grants (2012M1A2A2671788, 2013M3C8A3078512, and 2011-0031643) through the National Research Foundation of Korea funded by the Ministry of Education, Science, and Technology. This work was partly supported by the GRRC program of Gyeonggi Province.

REFERENCES

(1) Sheng, K.; Sun, Y.; Li, C.; Yuan, W.; Shi, G. Ultrahigh-Rate Supercapacitors Based on Electrochemically Reduced Graphene Oxide for Ac Line-Filtering. *Sci. Rep.* **2012**, *2*, 247.

(2) El-Kady, M. F.; Strong, V.; Dubin, S.; Kaner, R. B. Laser Scribing of High-Performance and Flexible Graphene-Based Electrochemical Capacitors. *Science* **2012**, *335*, 1326−1330.

(3) Brousse, T.; Taberna, P.; Crosnier, O.; Dugas, R.; Guillemet, P.; Scudeller, Y.; Zhou, Y.; Favier, F.; Bélanger, D.; Simon, P. Long-term Cycling Behavior of Asymmetric Activated Carbon/MnO_2 Aqueous Electrochemical Supercapacitor. *J. Power Sources* **2007**, *173*, 633−641.

(4) Niu, Z.; Chen, J.; Hng, H. H.; Ma, J.; Chen, X. A Leavening Strategy to Prepare Reduced Graphene Oxide Foams. *Adv. Mater.* **2012**, *24*, 4144−4150.

(5) Luo, J.; Jang, H. D.; Huang, J. Effect of Sheet Morphology on the Scalability of Graphene-Based Ultracapacitors. *ACS Nano* **2013**, *7*, 1464−1471.

(6) Li, X.; Zhao, T.; Wang, K.; Yang, Y.; Wei, J.; Kang, F.; Wu, D.; Zhu, H. Directly Drawing Self-Assembled, Porous, and Monolithic Graphene Fiber from Chemical Vapor Deposition Grown Graphene Film and Its Electrochemical Properties. *Langmuir* **2011**, *27*, 12164−12171.

(7) He, Y.; Chen, W.; Li, X.; Zhang, Z.; Fu, J.; Zhao, C.; Xie, E. Free-Standing Three-Dimensional Graphene/MnO_2 Composite Networks as Ultra-Light and Flexible Supercapacitor Electrodes. *ACS Nano* **2013**, *7*, 174−182.

(8) Jung, N.; Kwon, S.; Lee, D.; Yoon, D.; Park, Y. M.; Benayad, A.; Choi, J.; Park, J. S. Synthesis of Chemical Bonded Graphene/Carbon Nanotube Composites and Their Application in Large Volumetric Capacitance Supercapacitors. *Adv. Mater.* **2013**, *25*, 6854−6858.

(9) Simon, P.; GogotSi, Y. Materials for Electrochemical Capacitors. *Nat. Mater.* **2008**, *7*, 845−854.

(10) Gao, W.; Singh, N.; Song, L.; Liu, Z.; Reddy, A. L. M.; Ci, L.; Vajtai, R.; Zhang, Q.; Wei, B.; Ajayan, P. M. Direct Laser Writing of Micro-Supercapacitors on Hydrated Graphite Oxide Films. *Nat. Nanotechnol.* **2011**, *6*, 496−500.

(11) Pech, D.; Brunet, M.; Durou, H.; Huang, P.; Mochalin, V.; Gogotsi, Y.; Taberna, P.; Simon, P. Ultrahigh-Power Micrometre-Sized Supercapacitors Based on Onion-Like Carbon. *Nat. Nanotechnol.* **2010**, *5*, 651.

(12) Wang, M.; Oh, J.; Ghosh, T.; Hong, S.; Nam, G.; Hwang, T.; Nam, J. An Interleaved Porous Laminate Composed of Reduced Graphene Oxide Sheets and Carbon Black Spacers by in situ Electrophoretic Deposition. *RSC Adv.* **2014**, *4*, 3284−3292.

(13) Yoo, J. J.; Balakrishnan, K.; Huang, J.; Meunier, V.; Sumpter, B. G.; Srivastava, A.; Conway, M.; Reddy, A. L. M.; Yu, J.; Vajtai, R.;

DOI: 10.1021/am507656q
ACS Appl. Mater. Interfaces 2015, 7, 1348−1354

Ajayan, P. M. Ultrathin Planar Graphene Supercapacitors. *Nano Lett.* **2011**, *11*, 1423−1427.
(14) Oh, J.; Hwang, T.; Nam, G.; Hong, J.; Bae, A.; Son, S.; Lee, G.; Sung, H. K.; Choi, H. R.; Koo, J. C.; Nam, J. Chemically-Modified Graphene Sheets as An Active Layer for Ecofriendly Metal Electroplating on Plastic Substrates. *Thin Solid Films* **2012**, *521*, 270−274.
(15) Ghosh, T.; Biswas, C.; Oh, J.; Arabale, G.; Hwang, T.; Luong, N. D.; Jin, M.; Lee, Y. H.; Nam, J. Solution-Processed Graphite Membrane from Reassembled Graphene Oxide. *Chem. Mater.* **2012**, *24*, 594.
(16) Kaempgen, Martti; Chan, C. K.; Ma, J.; Cui, Y.; Gruner, G. Printable Thin Film Supercapacitors Using Single-Walled Carbon Nanotubes. *Nano Lett.* **2009**, *9* (5), 1872−1876.
(17) Wang, M.; Duong, L. D.; Oh, J.; Mai, N. T.; Kim, S.; Hong, S.; Hwang, T.; Lee, Y.; Nam, J. Large-Area, Conductive and Flexible Reduced Graphene Oxide (RGO) Membrane Fabricated by Electrophoretic Deposition (EPD). *ACS Appl. Mater. Interfaces* **2014**, *6*, 1747−1753.
(18) Meher, S. K.; Rao, G. R. Ultralayered Co_3O_4 for High-Performance Supercapacitor Applications. *J. Phys. Chem. C* **2011**, *115*, 15646−15654.
(19) Lin, J.; Zhang, C.; Yan, Z.; Zhu, Y.; Peng, Z.; Hauge, R. H.; Natelson, D.; Tour, J. M. 3-Dimensional Graphene Carbon Nanotube Carpet-Based Microsupercapacitors with High Electrochemical Performance. *Nano Lett.* **2013**, *13*, 72−78.
(20) Moon, G. D.; Joo, J. B.; Yin, Y. Stacked Multilayers of Alternating Reduced Graphene Oxide and Carbon Nanotubes for Planar Supercapacitors. *Nanoscale* **2013**, *5*, 11577−11581.
(21) Zhang, L.; Zhang, F.; Yang, X.; Long, G.; Wu, Y.; Zhang, T.; Leng, K.; Huang, Y.; Ma, Y.; Yu, A.; Chen, Y. Porous 3D Graphene-Based Bulk Materials with Exceptional High Surface Area and Excellent Conductivity for Supercapacitors. *Sci. Rep.* **2013**, *3*, 1408.
(22) Kim, T.; Jung, G.; Yoo, S.; Suh, K. S.; Ruoff, R. S. Activated Graphene-Based Carbon as Supercapacitor Electrodes with Macro- and Mesopores. *ACS Nano* **2013**, *7*, 6899−6905.
(23) Chang, J.; Jin, M.; Yao, F.; Kim, T. H.; Le, V. T.; Yue, H.; Gunes, F.; Li, B.; Ghosh, A.; Xie, S.; Lee, Y. H. Asymmetric Supercapacitors Based on Graphene/MnO_2 Nanospheres and Graphene/MoO_3 Nanosheets with High Energy Density. *Adv. Funct. Mater.* **2013**, *23*, 5074−5083.
(24) Jung, H. Y.; Karimi, M. B.; Hahm, M. G.; Ajayan, P. M.; Jung, Y. J. Transparent, Flexible Supercapacitors from Nano-Engineered Carbon Films. *Sci. Rep.* **2012**, *2*, 773.
(25) Niu, C.; Sichel, E. K.; Hoch, R.; Moy, D.; Tennent, H. High Power Electrochemical Capacitors Based on Carbon Nanotube Electrodes. *Appl. Phys. Lett.* **1997**, *70*, 1480.
(26) Li, X.; Zang, X.; Li, Z.; Li, X.; Li, P.; Sun, P.; Lee, X.; Zhang, R.; Huang, Z.; Wang, K.; Wu, D.; Kang, F.; Zhu, H. Large-Area Flexible Core-Shell Graphene/Porous Carbon Woven Fabric Films for Fiber Supercapacitor Electrodes. *Adv. Funct. Mater.* **2013**, *23*, 4862−4869.
(27) Xu, Y.; Lin, Z.; Huang, X.; Liu, Y.; Huang, Y.; Duan, X. Flexible Solid-State Supercapacitors Based on Three-Dimensional Graphene Hydrogel Films. *ACS Nano* **2013**, *7*, 4042−4049.

DOI: 10.1021/am507656q
ACS Appl. Mater. Interfaces 2015, 7, 1348−1354